DETECTABILITY OF SUMMER DRYNESS CAUSED BY GREENHOUSE WARMING

R. T. WETHERALD
Geophysical Fluid Dynamics Laboratory/NOAA, Forrestal Campus, Forrestal Road/US Route 1, P.O. Box 308, Princeton, NJ 08542, U.S.A.

SYUKURO MANABE
Institute for Global Change Research/FRSGC, Tokyo, Japan

Abstract. This study investigates the temporal and spatial variation of soil moisture associated with global warming as simulated by long-term integrations of a coupled ocean-atmosphere model conducted earlier. Starting from year 1765, integrations of the coupled model for 300 years were performed for three scenarios: increasing greenhouse gases only, increasing sulfate-aerosol loading only and the combination of both radiative forcings. The integration with the combined radiative forcings reproduces approximately the observed increases of global mean surface air temperature during the 20th century. Analysis of this integration indicates that both summer dryness and winter wetness occur in middle-to-high latitudes of North America and southern Europe. These features were identified in earlier studies. However, in the southern part of North America where the percentage reduction of soil moisture during summer is quite large, soil moisture is decreased for nearly the entire annual cycle in response to greenhouse warming. A similar observation applies to other semi-arid regions in subtropical to middle latitudes such as central Asia and the area surrounding the Mediterranean Sea. On the other hand, annual mean runoff is greatly increased in high latitudes because of increased poleward transport of moisture in the warmer model atmosphere.

An analysis of the central North American and southern European regions indicates that the time when the change of soil moisture exceeds one standard deviation about the control integration occurs considerably later than that of surface air temperature for a given experiment because the ratio of forced change to natural variability is much smaller for soil moisture compared with temperature. The corresponding lag time for runoff change is even greater than that of either precipitation or soil moisture for the same reason. Also according to the above criterion, the inclusion of the effect of sulfate aerosols in the greenhouse warming experiment delays the noticeable change of soil moisture by several decades. It appears that observed surface air temperature is a better indicator of greenhouse warming than hydrologic quantities such as precipitation, runoff and soil moisture. Therefore, we are unlikely to notice definitive CO_2-induced continental summer dryness until several decades into the 21st century.

1. Introduction

Recently, Haywood et al. (1997), investigated the responses of a coupled ocean-atmosphere model, developed at the Geophysical Fluid Dynamics Laboratory (GFDL) of NOAA, to increases of not only anthropogenic greenhouse gases but also sulfate aerosols. In particular, they briefly described the changes of mid-latitude continental soil moisture during the summer season as obtained from the

Climatic Change **43:** 495–511, 1999.

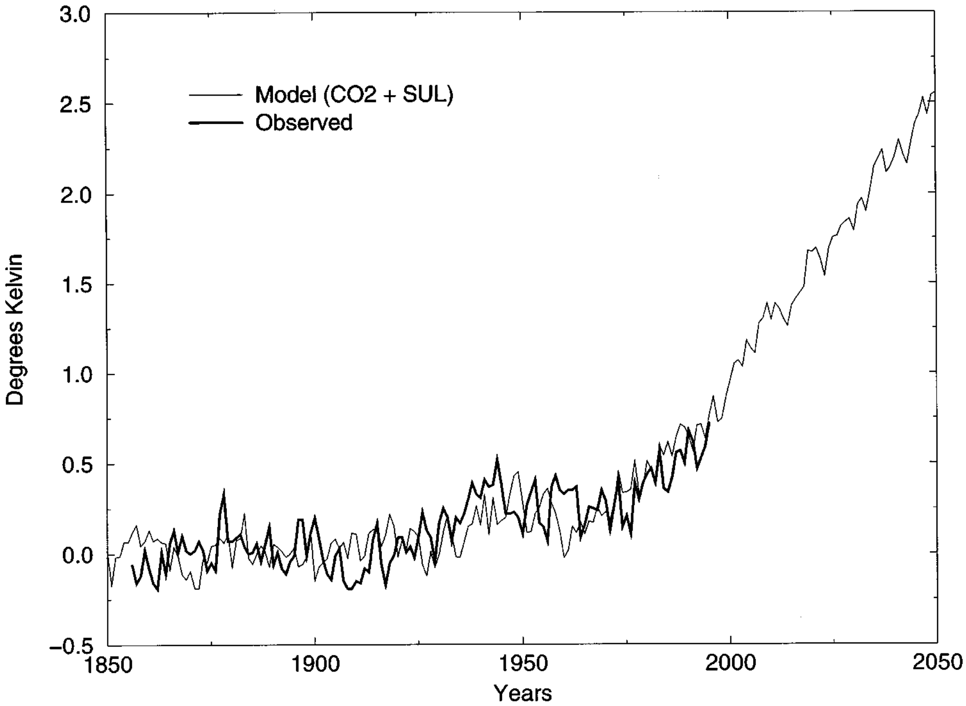

Figure 1. The time series of globally averaged annual mean surface air temperature anomaly (K) for the GFDL R15 coupled ocean-atmosphere model for 'CO_2 + SUL' (thin line) and corresponding observed anomaly defined as the deviation from the 1880–1920 average (thick line) (Jones and Briffa, 1992). This figure is from Figure 1 of Haywood et al. (1997).

coupled model. They concluded that, owing to reflection of insolation by increasing sulfate aerosols and the large inter-annual variability of soil moisture amount, a summer dryness signal does not become apparent until after the beginning of the 21st century in the experiment with both greenhouse gases and aerosols. The present study will describe and discuss these changes in greater detail.

At present, there are large uncertainties in the magnitude of the thermal forcing of sulfate aerosols as well as ignorance of other anthropogenic and natural factors which may have forced climate over the past 200 years. Nevertheless, the model including both sulfate aerosols and greenhouse gases simulates, approximately, the warming trend during this century (Figure 1). This encouraged us to evaluate the mid-latitude continental summer dryness which appears during the early part of the next century in the numerical experiment discussed by Haywood et al. (1997) and Manabe (1998).

Using simpler general circulation models in which the atmosphere is connected to a mixed-layer ocean model, several investigators found that soil moisture tends to decrease during the summer season over mid-continental regions in middle and high latitudes in response to an increase of atmospheric carbon dioxide concentration (e.g., Manabe et al., 1981; Manabe and Wetherald, 1987; Mitchell and Warrilow, 1987). These results are summarized in Schlesinger and Mitchell (1987), Kellogg and Zhao (1988) and Mitchell et al. (1990). This tendency for continental summer drying has also been obtained in 'coupled model' experiments such as Manabe et al. (1992), Gregory et al. (1997) and Mitchell and Johns (1997). Using a mixed-layer model with highly idealized geography, Wetherald and Manabe (1995) (hereafter WM95) investigated the specific mechanisms responsible for the summer dryness.

This study will attempt to answer the following questions.

a) How is the soil moisture change of the coupled model altered if the cooling effect of increasing sulfate aerosols is added to the warming effect of increasing greenhouse gases?
b) When will the soil moisture change associated with global warming become large enough to be noticeable?
c) What are the physical mechanisms for the changes in soil moisture and runoff associated with global warming?

It is likely that the systematic changes of soil moisture discussed in this study could have an important impact on agricultural practices and other human activities. Although soil moisture is not a variable which is routinely observed, we believe that it is worthwhile to inquire when the changes of soil moisture, as well as other hydrologic quantities, become large enough to be notable.

2. Model Description and Experimental Procedure

Since our analysis uses the integrations described in Haywood et al. (1997), only a brief outline of the model and experimental procedure is given here. The coupled ocean-atmosphere land-surface model of Manabe et al. (1991) was used, which is constructed by combining a general circulation model of the world ocean with a general circulation model of the atmosphere. The atmospheric model is a spectral model, rhombiodally truncated at wave number 15 (R15), which includes global geography, seasonally varying radiative processes, and heat and water budgets at the continental surface. Overcast cloud is forecast whenever the relative humidity exceeds 99%; otherwise clear sky is assumed.

Hydrologic processes are simulated according to the scheme described in Manabe (1969). Over the continents, both snow cover and soil moisture are predicted. Snow cover is determined from snowfall, sublimation and snowmelt. Soil moisture is computed by the 'bucket method' where the soil is assumed to have a water holding capacity of 15cm. If the computed soil moisture exceeds this amount, the excess is classified as runoff. Changes in soil moisture are computed from the rates of rainfall, evaporation, snowmelt and runoff. Evaporation from the soil surface is determined as a function of soil moisture and the potential evaporation rate.

The effects of both aerosols and greenhouse gases were incorporated into the above model. In particular, estimates of past, present and future equivalent carbon dioxide and sulfate concentrations are identical to those of Mitchell et al. (1995a,b). Here, the equivalent carbon dioxide concentration is prescribed for years 1765 to 1990 (Mitchell et al., 1995a), followed by a 1% per year increase compounded for years 1990 to 2065. The direct radiative forcing of sulfate aerosols is simulated by adjusting the surface reflectance of solar radiation according to the method of Mitchell et al. (1995a,b). This scheme simply parameterizes the reflective effects of aerosols without performing the radiative computations on the three-dimensional distributions of aerosols directly. The actual aerosol distribution for each model year is determined from separate loading patterns for the years 1986 and 2050, following the scenario IS92a of the report IPCC-1992 (Leggett et al., 1992). It is interpolated from a zero loading pattern at 1765 to the loading pattern at 1986, linearly interpolated between the two loading patterns for years 1986 to 2050, then extrapolated from the loading pattern of 2050 to 2065.

As stated in Haywood et al. (1997), four separate integrations are performed:

i. A 1000-year control integration where the equivalent CO_2 concentrations of greenhouse gases (except water vapor) and sulfate aerosols are held fixed at year 1765 levels.
ii. A greenhouse-gas forcing only (referred to as 'CO_2'),
iii. Sulfate-aerosol forcing only (referred to as 'SUL'),
iv. Both the equivalent carbon dioxide and sulfate aerosol forcings stated above for years 1765 to 2065 (referred to as $CO_2 + SUL$).

In the subsequent discussion, the above acronyms will indicate the difference between each experiment and the control integration (i.e., CO_2 means CO_2 minus control, etc.). A detailed analysis is made of two specific regions taken from the report IPCC-1990 (Mitchell et al., 1990), namely, central North America (CNA, 35–50 N, 85–105 W) and southern Europe (SEU, 35–50 N, 10 W–45 E). These regions are chosen for their importance in agriculture.

3. Response of Surface Hydrology

3.1. JUNE–JULY–AUGUST RESPONSE

A natural starting point for this analysis is the global response of soil moisture obtained from the '$CO_2 + SUL$' experiment for the summer (June–July–August) season. During years 1985–2015, the change of soil moisture is relatively small except for an apparent negative maximum region over central Canada (Figure 2a) which almost disappears later (Figure 2b). However, more definitive changes occur in years 2035–2065 when soil moisture decreases over most continental regions, especially North America, Europe and central Asia (Figure 2b). Although this feature has been present in previous studies (e.g., Manabe and Wetherald, 1987;

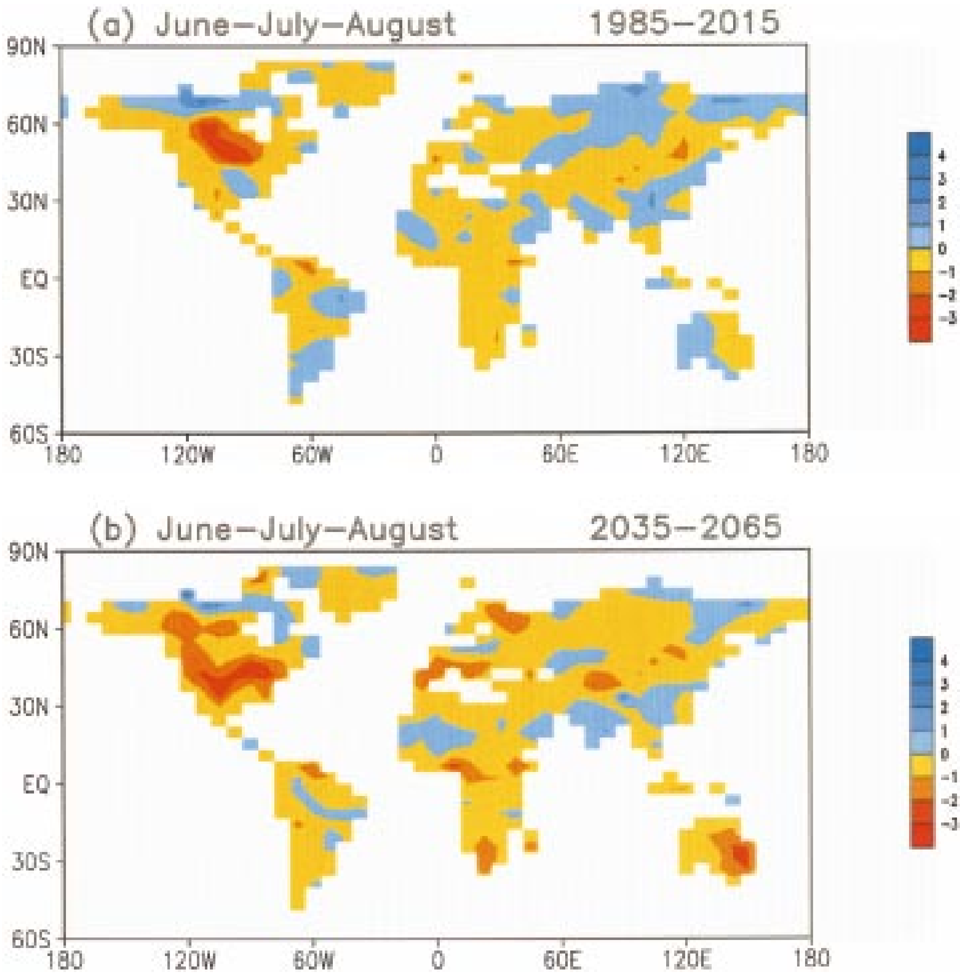

Figure 2. (a) Geographical distribution of the difference in soil moisture (cm) between the 'CO_2 + SUL' and control experiments averaged over June–July–August for years 1985–2015. (b) Same as above except for years 2035–2065. Differences here and all other figures are computed using the 1000-year mean values from the control integration.

Manabe et al., 1992), it does not become apparent in 'CO_2 + SUL' until two to three decades into the next century. Over India, soil moisture actually increased during the summer season due to enhanced monsoonal rainfall there. This result has appeared consistently also in earlier studies (e.g., Mitchell et al., 1990).

The relative importance of the soil moisture changes shown in Figure 2b can be evaluated by referring to the percentage change shown in Figure 3. (Percentage change is defined as the CO_2-induced change in Figure 2b divided by the soil moisture from the control run.) In this figure, the percentage reduction of soil moisture exceeds 30% for the southwestern portion of North America, central Asia and the regions surrounding the Mediterranean Sea. In the Southern Hemisphere, it is also

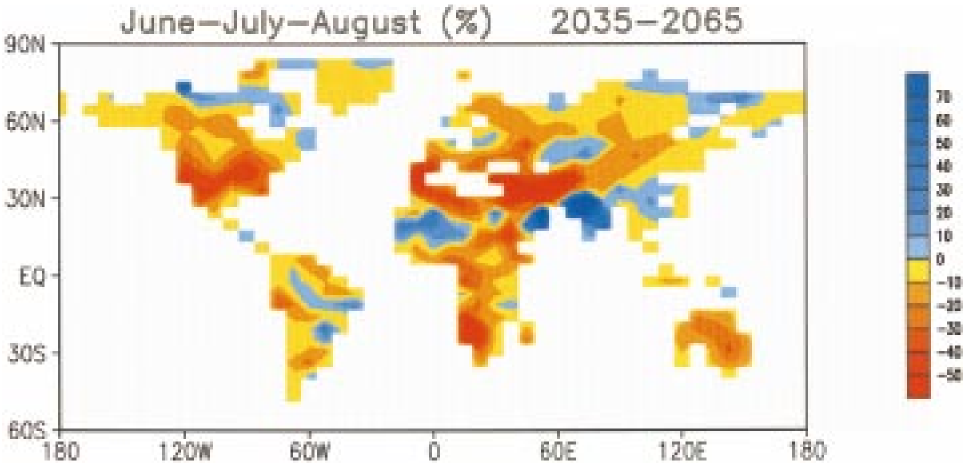

Figure 3. Geographical distribution of the percentage (%) of the soil moisture difference represented in Figure 2b to the time mean values of soil moisture from the control integration.

quite large in Australia and the southern portion of Africa. In general, the greatest percentage reductions occur in semi-arid regions of subtropical latitudes where the amount of soil moisture in the control run is relatively small and the insolation is quite large. The percentage reductions of soil moisture are quite small in higher latitudes where the soil is nearly saturated in the control run. As noted above, an exception to this general drying is India where the percentage increases of soil moisture are 50 to 70%.

In order to evaluate the detectability of soil moisture changes which occur in response to the various radiative forcings, the magnitudes of the soil moisture changes are compared with the standard deviation of the natural soil moisture variability in the control integration. When the forced change (i.e., signal) exceeds the standard deviation of the natural variability (i.e., noise), it is likely that we can distinguish the signal from the noise. In other words, the signal becomes 'detectable'. (Hereafter, the term 'detectable' will be used in this manner for the sake of convenience). Figures 4a and 4b illustrate, for the CNA and SEU regions respectively, the smoothed time series of 20 year running-mean values of summer soil moisture anomalies together with the standard deviation of soil moisture from the control integration. These figures indicate that the appearance of a detectable change of soil moisture in '$CO_2 + SUL$' lags that in 'CO_2' by about 20 years for both regions. In CNA, the reduction of soil moisture does not become detectable until approximately year 2010 in 'CO_2' and year 2030 in '$CO_2 + SUL$'. In SEU, a similar difference exists between 'CO_2' and '$CO_2 + SUL$'.

The change of surface air temperature becomes detectable much earlier than that of soil moisture. Figure 5 illustrates the corresponding time series of yearly mean anomalies of surface air temperature averaged over June-July-August for CNA and SEU. In '$CO_2 + SUL$' for example, a change of surface air temperature becomes

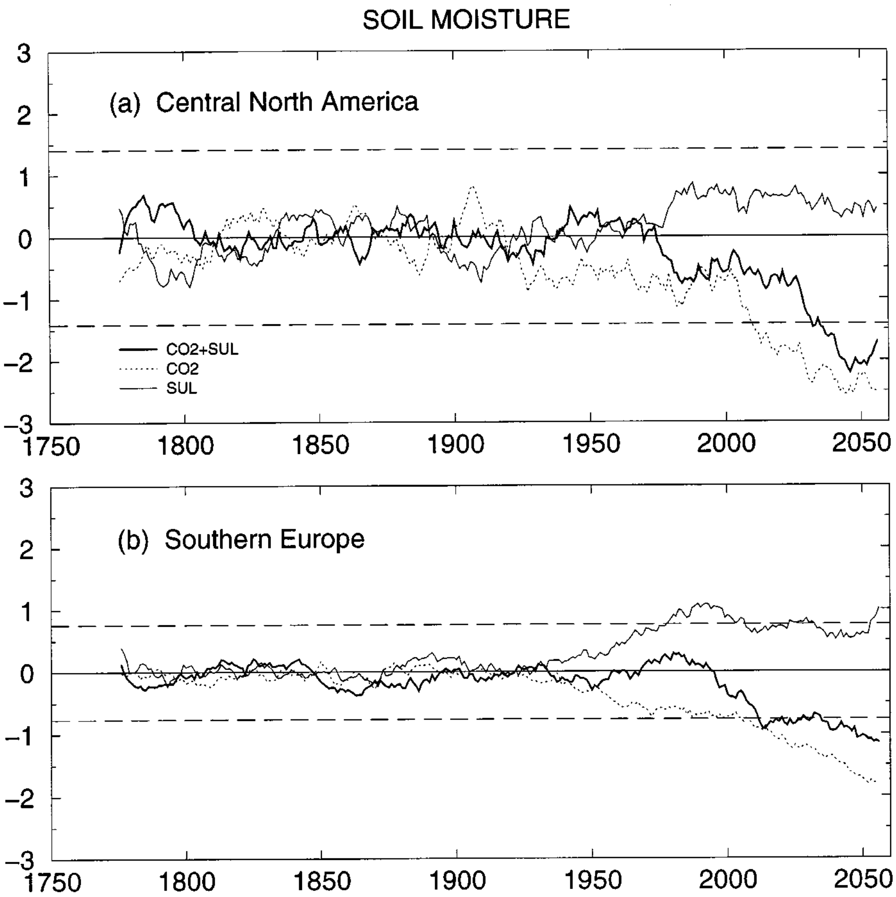

Figure 4. Time series of area-averaged soil moisture anomaly (cm) for the 'CO_2 + SUL', 'CO_2' and 'SUL' experiments for the regions (a) CNA and (b) SEU. Each time series consists of differences between the yearly June–July–August averages of soil moisture for each of the three integrations and the corresponding control integration over the entire 1000-year period for June–July–August. Each time series has been smoothed by a 20 year running mean. The two horizontal dashed lines denote one standard deviation limits from the control integration computed from the yearly June–July–August averages.

detectable as early as year 1975. For both 'CO_2' and 'CO_2 + SUL', the appearance of a detectable change of soil moisture lags behind that of surface air temperature by several decades in both the CNA and SEU regions (compare Figures 4 and 5). This is because the signal-to-noise ratio for soil moisture is much smaller than that for surface air temperature. This smaller signal-to-noise ratio of soil moisture is attributable to the relatively large natural variability of the yearly mean change of precipitation rate (not shown). Figures 4 and 5 also indicate that the inclusion of aerosols delays the detectable changes of both soil moisture and temperature

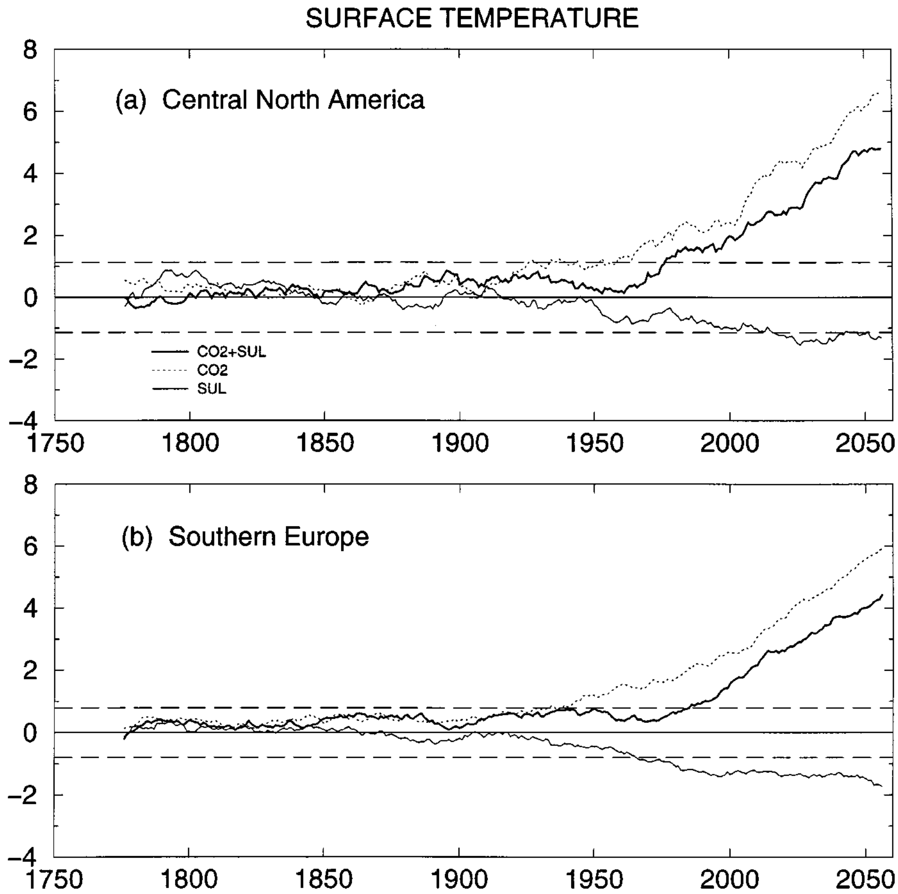

Figure 5. Same as Figure 4 except for surface air temperature (degrees C).

by several decades. This suggests that definitive evidence of CO_2-induced summer drying in these locations may not appear until several decades into the 21st century.

3.2. DECEMBER–JANUARY–FEBRUARY RESPONSE

During winter, soil moisture increases in middle to higher latitudes of the Northern Hemisphere as indicated in Figure 6b. In high latitudes, the increase of soil moisture becomes significant during the years 1985–2015 (Figure 6a). In middle latitudes there is relatively little consistent change of soil moisture in years 1985–2015 whereas a more definitive change occurs in years 2035–2065 (Figure 6b). This CO_2-induced increase of soil moisture over the continents in middle to high latitudes has occurred in previous studies (e.g., Manabe and Wetherald, 1987; Manabe et al., 1992). Also, in the southern and central portions of the U.S., soil moisture is decreased in both summer and winter, which implies that drier conditions exist there throughout the entire year. Similar conditions apply to other regions, such as

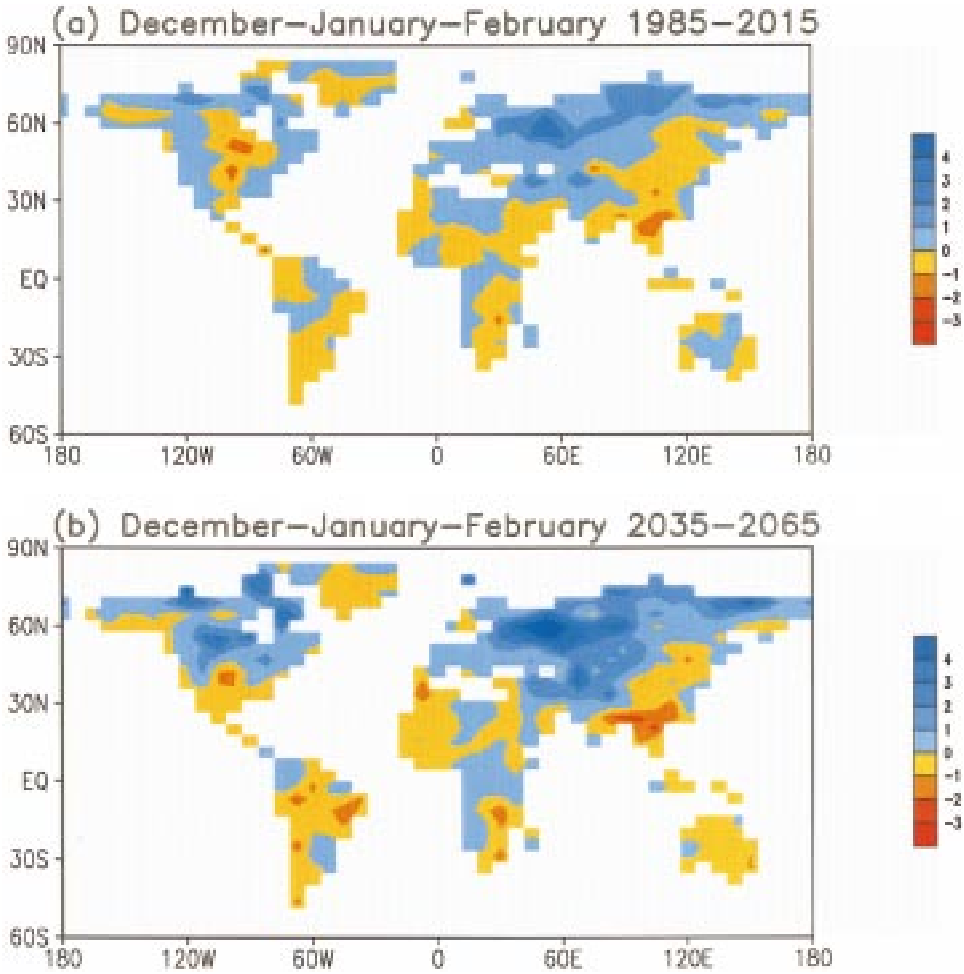

Figure 6. (a) Geographical distribution of soil moisture anomaly (cm) from 'CO_2 + SUL' during December–January–February for years 1985–2015. (b) Same as (a) except for years 2035–2065.

central Asia and the area surrounding the Mediterranean Sea. This topic will be discussed further in Section 4.

3.3. ANNUAL MEAN RESPONSE

As an example of the annual mean response of hydrology in 'CO_2 + SUL', Figure 7 shows the difference of runoff for years 2035–2065. Relatively large increases of annual mean runoff occur in the higher latitudes of North America, Europe and Eurasia. Manabe and Wetherald (1975, 1980), showed that greenhouse warming produced a larger poleward transport of water vapor resulting in a marked increase of precipitation in higher latitudes. Since the soil moisture of the control run is nearly saturated in higher latitudes, most of this increased precipitation is trans-

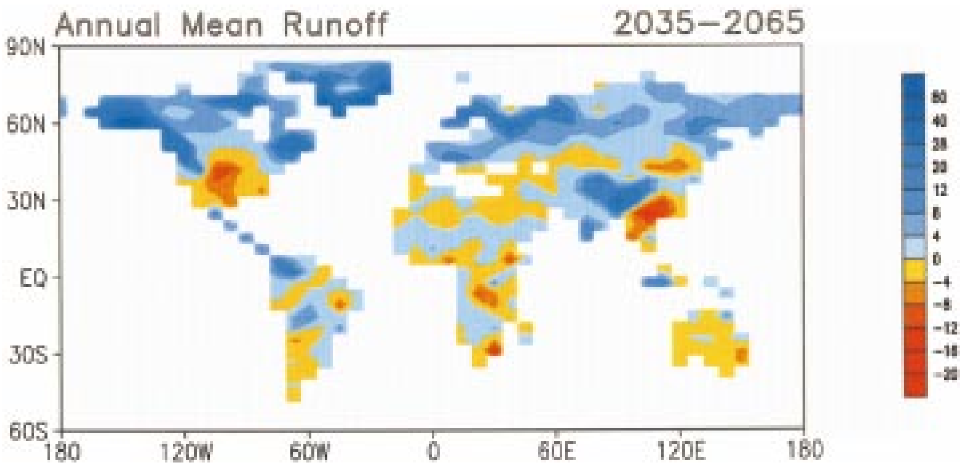

Figure 7. Geographical distribution of the annual mean runoff anomaly (cm/year) from 'CO_2 + SUL' for the time period 2035–2065.

lated directly into increases of runoff through both rainfall and snowmelt (Manabe and Wetherald, 1987). These results indicate that, although drier conditions occur during the summer season over the continents of the Northern Hemisphere due to greenhouse warming, the surplus of precipitation and snowmelt during the rest of the year compensates for this summer dryness over most regions and provides more runoff overall. An exception is the central and southern portions of the U.S., where the annual mean runoff is decreased. In the subtropical regions of Eurasia and Africa, there is a slight reduction in annual mean runoff except for India and Tibet where both runoff and soil moisture are increased greatly (Figure 7, Figure 2b), respectively.

Figure 8 shows the distributions of yearly runoff differences obtained from the three experiments during June–July–August for both CNA and SEU. Here, the decreased runoff change for 'CO_2' becomes detectable around the year 2030 for both regions, whereas the corresponding changes of runoff are not detectable for either 'CO_2 + SUL' or 'SUL' throughout their entire integrations. Since in general, runoff has a smaller signal to noise ratio than soil moisture, more time is required to obtain detectable differences for this quantity. Therefore, detectable changes of runoff lag those of both soil moisture and surface temperature.

4. Mechanism of Summer Dryness

As described already, soil moisture in the mid-continental regions of the coupled model is reduced in summer during the first half of the 21st century ('CO_2 + SUL'). The percentage reduction of soil moisture, however, is particularly large in semi-arid regions of the world, such as the southern part of North America, central

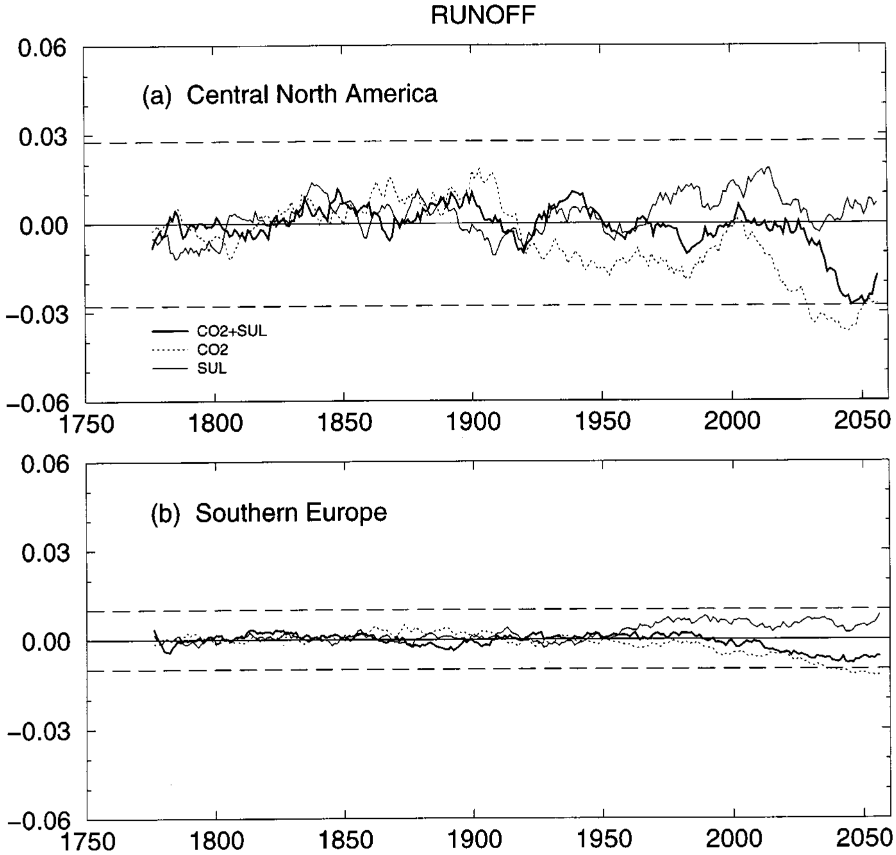

Figure 8. Time series of area averaged annual mean runoff anomaly (cm/day) for the 'CO_2 + SUL', 'CO_2' and 'SUL' experiments, respectively, for the regions of (a) CNA and (b) SEU. Otherwise, same as Figure 4.

Asia and the area around the Mediterranean Sea. In these regions, soil moisture is reduced during most of the year, in contrast to middle and higher latitude regions where soil moisture is increased in winter and reduced during summer.

In order to explore the physical mechanisms responsible for the CO_2-induced change in soil moisture, we highlight two separate regions in the North American Continent of the coupled model. In the northern region, named CNA1 (40–53° N, 85–105° W), soil moisture is decreased in summer but increased markedly in winter. On the other hand, soil moisture is decreased during most of the year in the southern region, named CNA2 (27–40° N, 85–105° W). Because the mechanisms of soil moisture change are significantly different between these two regions, these mechanisms are discussed separately.

For the CNA1 region, the annual cycles of soil moisture for the 'CO_2 + SUL' and control integrations are presented in Figure 9a. These cycles are averaged over the last 30 years (i.e., 2035–2065) of the integration. In CNA1, where the soil moisture

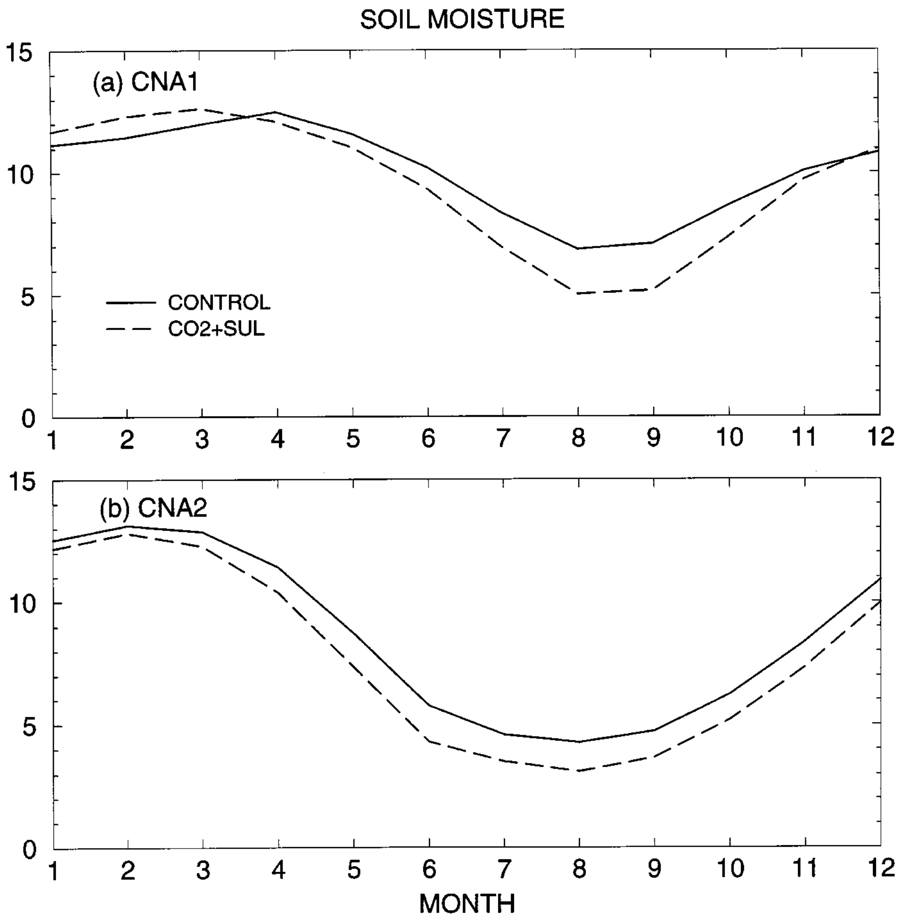

Figure 9. Seasonal variation of the monthly mean soil moisture from the 'CO_2 + SUL' and the control integrations taken over the period of 2035–2065 for the (a) CNA1 region and (b) CNA2 region. Units are in cm.

often approaches saturation in spring, the change of soil moisture associated with global warming becomes negative from spring to fall, whereas it is positive in winter (Figure 9a). Since the mechanisms responsible for the summer reduction of soil moisture in this type of region were discussed extensively in previous studies (i.e., Manabe and Wetherald, 1987; MW95), they will simply be outlined here as follows.

In general, the increase of both CO_2 and water vapor in the model atmosphere increases the downward flux of longwave radiation absorbed by the continental surface. This results in an early disappearance of snow cover (with a large surface albedo), thereby increasing the solar energy absorbed by the continental surface. Because of the increase in the surface absorption of both longwave and solar radiation, evaporation is enhanced during spring and early summer (Figure 10a),

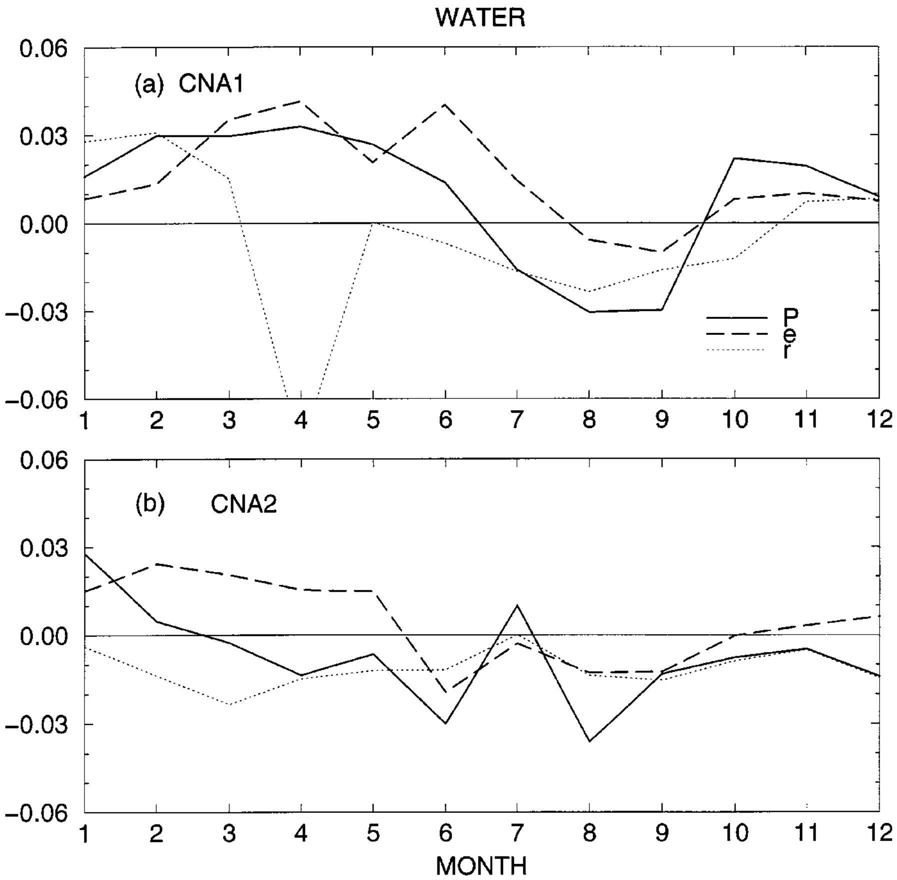

Figure 10. Seasonal variation of the difference in monthly mean rate of precipitation (P; solid line), that of evaporation (e; dashed line) and that of runoff (r; thin dotted line) obtained from the 'CO_2 + SUL' experiment. The rates represent the averages during the period of 2035–2065 over (a) CNA1 region and (b) CNA2 region. Units are in cm/day.

reducing the soil moisture in the CNA1 region. By mid-summer, the soil moisture is reduced to the point where evaporation can no longer increase. Thus, evaporation is decreased and sensible heat increased, reducing the near-surface relative humidity and cloud cover, which increases insolation absorbed by the continental surface and makes more energy available for evaporation. On the other hand, the rate of precipitation hardly increases over the continents in summer because of the low relative humidity in the lower troposphere (Figure 10a). As a matter of fact, the rate of precipitation even decreases slightly after mid-summer when the soil becomes very dry. Therefore, the soil moisture anomaly remains negative throughout the rest of the summer and early fall in 'CO_2 + SUL'.

In sharp contrast to the summer situation discussed above, soil moisture in CNA1 increases during winter in 'CO_2 + SUL' (Figure 9a). Despite the increase in the downward flux of longwave radiation, the rate of evaporation hardly increases over the continental surface in middle and high latitudes where the increase in the downward flux is compensated mainly by the upward fluxes of sensible heat and longwave radiation rather than latent heat flux in winter. On the other hand, the rate of precipitation increases significantly in the CNA1 region where the relative humidity in the lower troposphere is much higher in winter than in summer (Figure 10a). This is quite different from the situation in summer when the relative humidity in the lower troposphere is very low and precipitation hardly increases in this region despite the increase in the rate of evaporation in the surrounding oceans. The increase in precipitation, together with the failure of evaporation to increase, accounts for the increase of soil moisture in the CNA1 region during winter in 'CO_2 + SUL'.

In the CNA2 region, where there is little or no snow cover in spring, the monthly mean soil moisture is considerably below saturation during most of the year. Figure 9b indicates that the CO_2-induced change in soil moisture is negative throughout the entire year and the maximum reduction occurs from summer to early winter. As in CNA1, the reduction of soil moisture in CNA2 is attributable partly to the increased downward flux of terrestrial radiation resulting from the increase of both CO_2 and water vapor in the model atmosphere.

The increase in the downward flux of longwave radiation raises the surface temperature, thereby increasing the rate of potential evaporation. As Figure 10b indicates, the increase in potential evaporation increases the evaporation from early winter to May when the soil moisture is relatively large. However, the CO_2-induced change in the evaporation rate becomes slightly negative from summer to early fall when soil moisture is relatively small. On the other hand, the CO_2-induced change of precipitation rate in the CNA2 region is negative throughout most of the annual cycle (Figure 10b), in sharp contrast to the situation over most of the globe where both evaporation and precipitation increase in response to the increasing atmospheric carbon dioxide. The failure of precipitation to increase is attributable partly to the reduction of near-surface relative humidity in these regions where a major fraction of radiative energy absorbed at the land surface is removed as sensible heat flux rather than through evaporation. The increase in potential evaporation together with the reduction of precipitation discussed above contribute to the general reduction of soil moisture shown in Figure 9b. The decrease of soil moisture, in turn, reduces the near-surface relative humidity and precipitation rate further throughout most of the year (Figure 10b). The reduced near-surface relative humidity induces a corresponding reduction of low level cloudiness, increasing the insolation reaching the continental surface and further enhancing the drying of the soil. This analysis applies equally well to other semi-arid regions of the world such as central Asia and the area surrounding the Mediterranean Sea.

5. Summary and Conclusions

Results of the 'CO_2 + SUL' integration suggest that, over mid-continental regions of middle and high latitudes, the summer reduction and winter increase of soil moisture will not become noticeable until the first half of the 21st century. An analysis of the central North American and southern European regions indicates that the time when the change of soil moisture exceeds one standard deviation about the control integration occurs considerably later than that of surface temperature because the ratio of the forced change to the natural variability is smaller for soil moisture than for temperature. It is also found that the cooling effect of sulfate aerosols delays the detection of both soil moisture and surface temperature changes by several decades.

The percentage reduction of soil moisture in summer is particularly large in some semi-arid regions of the subtropical to middle latitudes, such as the southern part of North America, central Asia and the areas around the Mediterranean Sea. In these regions, soil moisture is reduced during most of the year, in contrast to the mid-continental regions of middle-to-higher latitudes where soil moisture is reduced during summer but increased in winter. In south Africa and Australia of the Southern Hemisphere, the percentage reduction of soil moisture is pronounced in winter. In response to the increased downward flux of terrestrial radiation associated with greenhouse warming, surface temperature is increased markedly in these semi-arid regions, which increases potential evaporation. On the other hand, the precipitation rate hardly increases or even decreases slightly in these regions where a major fraction of the additional radiative energy absorbed by the land surface is removed as sensible heat flux rather than through evaporation. Both of these factors contribute to reduced soil moisture during most of the annual cycle.

Annual mean precipitation and runoff are increased considerably in high latitudes of North America, Europe and Eurasia due to the greater poleward transport of water vapor in the warmer model atmosphere. Since the soil is nearly saturated in high latitudes in the control integration, most of this increased precipitation occurs as runoff. This implies an excess of annual mean runoff in most river basins in high latitudes for the current greenhouse warming scenario.

One should note that the results described here do not always coincide with those obtained from similar sets of numerical experiments conducted at other institutions. For example, in the study described by Mitchell and Johns (1997), summertime soil moisture also decreased over both North America and Europe when only greenhouse gases were increased. However, soil moisture increased over southern Europe in response to the combined radiative forcing of both greenhouse gases and sulfate aerosols. One can speculate that this difference is attributable to the larger global warming of the GFDL model as compared with the Hadley Center model. Because of the difference in sensitivity, the warming of the continental surfaces attained by the middle of the 21st century is larger in the GFDL model than in the Hadley Center model, resulting in more summer dryness in the former model. If one extended the time integration of the Hadley Center model beyond the middle of the 21st century, mid-continental summer dryness may become more discernible.

It has been noted that the response of soil moisture to greenhouse warming depends very much upon the simulated distribution of summertime soil moisture in the control experiment. For example, if soil moisture is very small over mid-continental regions in summer, then CO_2-induced summer reduction of soil moisture cannot occur (e.g., Meehl and Washington, 1988; Kellogg and Zhao, 1988; Rind et al., 1990). One should also recognize that the geographical distributions of radiatively forced changes of hydrologic variables can depend significantly upon the details of the land-surface scheme used (Chen et al., 1997). In view of the difference in the hydrologic response among various models, one should not take too literally the geographical distributions of the changes of soil moisture and runoff obtained in the current study.

The results from the numerical experiments conducted here indicate that the ratio of radiatively forced to internally generated changes is much smaller with hydrologic variables than with surface temperature, a conclusion unlikely to be model-dependent. This implies that the latter is a more reliable indicator for the detection of greenhouse warming than hydrologic quantities such as precipitation, runoff and soil moisture. It should also be noted that the 1%/year increase of CO_2-equivalent concentration of greenhouse gases, assumed after 1990 in the present experiments, appears to be larger than the rate observed so far (Houghton et al., 1996). Therefore, we are unlikely to convincingly identify summer dryness attributable to greenhouse warming until several decades into the next century.

Acknowledgements

The authors would like to thank R. J. Stouffer for making available the data from his coupled model experiments. Thanks are also due to T. Delworth, P. C. D. Milly, I. Held, M. J. Spelman, J. F. B. Mitchell and two anonymous reviewers who provided constructive revisions to the manuscript.

References

Chen, T. H., Henderson-Sellers, A., Milly, P. C. D., Pitman, A. J., Beljaars, A. C. M., Polcher, J., Abramopoulos, F., Boone, A., Chang, S., Chen, F., Dai, Y., Desborough, C. E., Dickinson, R. E., Dumenil, L., Ek, M., Garratt, J. R., Gedney, N., Gusev, Y. M., Kim, J., Koster, R., Kowalczyk, E. A., Lavel, K., Lean, J., Lettenmaier, D., Liang, X., Mahfouf, J.-F., Mengelkamp, H.-T., Mitchell, K., Nasonova, O. N., Noilhan, J., Robock, A., Rosenzweig, C., Schaake, J., Schlosser, C. A., Schulz, J.-P., Shao, Y., Shmakin, A. B., Verseghy, D. L., Wetzel, P., Wood, E. F., Xue, Y., Yang, Z.-L., and Zeng, Q.: 1997, 'Cabauw Experimental Results from the Project for Intercomparison of Land-Surface Parameterization Schemes', *J. Climate* **10**, 1194–1215.

Gregory, J. M., Mitchell, J. F. B., and Brady, A. J.: 1997, 'Summer Drought in Northern Mid-Latitudes in a Time-Dependent CO_2 Climate Experiment', *J. Climate* **10**, 662–686.

Haywood, J. M., Stouffer, R. J., Wetherald, R. T., Manabe, S., and Ramaswamy, V.: 1997, 'Transient Response of a Coupled Model to Estimated Changes in Greenhouse Gas and Sulfate Concentrations', *Geophys. Rev. Lett.* **24**, 1335–1338.

Houghton, J. T., Meira Filho, L. G., Callander, B. A., Harris, N., Kattenberg, A., and Maskell, K.: 1996, 'Climate Change 1995: The IPCC Second Scientific Assessment', Cambridge University Press, Cambridge, p. 572.

Jones, P. D. and Briffa, K. B.: 1992, 'Global Surface Air Temperature Variations during the Twentieth Century, Part I: Spatial, Temporal and Seasonal Details', *The Holocene* **2**, 165–179.

Kellogg, W. W. and Zhao, Z.-C.: 1988, 'Sensitivity of Soil Moisture to Doubling of Carbon Dioxide in Climate Model Experiments, Part I: North America', *J. Climate* **1**, 348–366.

Leggett, J., Pepper, W. J., and Swart, R. J.: 1992, 'Emission Scenarios for the IPCC: An Update', in Houghton, J. T., Callendar, B. A., and Varney, S. K. (eds.), *Climate Change: Supplementary Report to the IPCC Scientific Assessment*, Cambridge University Press, Cambridge, pp. 74–95.

Manabe, S.: 1969, 'Climate and the Ocean Circulation: I. The Atmospheric Circulation and the Hydrology of the Earth's Surface', *Mon. Wea. Rev.* **97**, 739–774.

Manabe, S.: 1998, 'Study of Global Warming by GFDL Climate Models', *Ambio* **27**, 182–186.

Manabe, S. and Wetherald, R. T.: 1975, 'The Effects of Doubling the CO_2 Concentration on the Climate of a General Circulation Model', *J. Atmos. Sci.* **32**, 3–15.

Manabe, S. and Wetherald, R. T.: 1980, 'On the Distribution of Climate Change Resulting from an Increase of CO_2 Content of the Atmosphere', *J. Atmos. Sci.* **37**, 99–118.

Manabe, S. and Wetherald, R. T.: 1987, 'Large-Scale Changes of Soil Wetness Induced by an Increase in Atmospheric Carbon Dioxide', *J. Atmos. Sci.* **44**, 1211–1235.

Manabe, S., Wetherald, R. T., and Stouffer, R. J.: 1981, 'Summer Dryness Due To an Increase of Atmospheric CO_2 Concentration', *Clim. Change* **3**, 347–386.

Manabe, S., Stouffer, R. J., Spelman, M. J., and Bryan, K.: 1991, 'Transient Responses of a Coupled Ocean-Atmosphere Model to Gradual Changes of Atmospheric CO_2, Part I: Annual Mean Response', *J. Climate* **4**, 785–818.

Manabe, S., Spelman, M. J., and Stouffer, R. J.: 1992, 'Transient Responses of a Coupled Ocean-Atmosphere Model to Gradual Changes of Atmospheric CO_2, Part II: Seasonal Response', *J. Climate* **5**, 105–126.

Meehl, G. A. and Washington, W. M.: 1988, 'A Comparison of Soil-Moisture Sensitivity in Two Global Climate Models', *J. Atmos. Sci.* **45**, 1476–1492.

Mitchell, J. F. B. and Johns, T. C.: 1997, 'On Modification of Global Warming by Sulfate Aerosols', *J. Climate* **10**, 245–267.

Mitchell, J. F. B. and Warrilow, D. A.: 1987, 'Summer Dryness in Northern Mid-latitudes Due To Increased CO_2', *Nature* **330**, 238–240.

Mitchell, J. F. B., Manabe, S., Meleshko, V., and Tokioka, T.: 1990, 'Equilibrium Climate Change and its Implications for the Future', in Houghton, J. T., Jenkins, G. T., and J. J. Ephraums (eds.), *Climate Change: IPCC Scientific Assessment*, Cambridge University Press, Cambridge, pp. 131–164.

Mitchell, J. F. B., Johns, T. C., Gregory, J. M., and Tett, S. F. B.: 1995a, 'Climate Responses to Increasing Level of Greenhouse Gases and Sulfate Aerosols', *Nature* **376**, 501–504.

Mitchell, J. F. B., Davis, R. A., Ingram, W. J., and Senior, C. A.: 1995b, 'On Surface Temperature, Greenhouse Gases and Aerosols: Models and Observations', *J. Climate* **8**, 2364–2386.

Rind, D., Goldberg, R., Hansen, J., Rosenzweig, C., and Ruedy, R.: 1990, 'Potential Evapotranspiration and the Likelihood of Future Drought', *J. Geophys. Res.* **95D**, 9983–10004.

Schlesinger, M. E. and Mitchell, J. F. B.: 1987, 'Climate Model Simulations of the Equilibrium Climate Response to Increased Carbon Dioxide', *Rev. Geophys.* **25**, 760–798.

Wetherald, R. T. and Manabe, S.: 1995, 'The Mechanisms of Summer Dryness Induced by Greenhouse Warming', *J. Climate* **8**, 3096–3108.

(Received 29 June 1998; in revised form 2 March 1999)